



**HAL**  
open science

## Illustrations of a microdamage model for laminates under oxidizing thermal cycling

G. Lubineau, D. Violeau, P. Ladevèze

► **To cite this version:**

G. Lubineau, D. Violeau, P. Ladevèze. Illustrations of a microdamage model for laminates under oxidizing thermal cycling. *Composites Science and Technology*, 2009, 69 (1), pp.3. 10.1016/j.compscitech.2007.10.042 . hal-00575237

**HAL Id: hal-00575237**

**<https://hal.science/hal-00575237>**

Submitted on 10 Mar 2011

**HAL** is a multi-disciplinary open access archive for the deposit and dissemination of scientific research documents, whether they are published or not. The documents may come from teaching and research institutions in France or abroad, or from public or private research centers.

L'archive ouverte pluridisciplinaire **HAL**, est destinée au dépôt et à la diffusion de documents scientifiques de niveau recherche, publiés ou non, émanant des établissements d'enseignement et de recherche français ou étrangers, des laboratoires publics ou privés.

## Accepted Manuscript

Illustrations of a microdamage model for laminates under oxidizing thermal cycling

G. Lubineau, D. Violeau, P. Ladevèze

PII: S0266-3538(07)00429-0  
DOI: [10.1016/j.compscitech.2007.10.042](https://doi.org/10.1016/j.compscitech.2007.10.042)  
Reference: CSTE 3878

To appear in: *Composites Science and Technology*

Received Date: 14 May 2007  
Accepted Date: 11 October 2007

Please cite this article as: Lubineau, G., Violeau, D., Ladevèze, P., Illustrations of a microdamage model for laminates under oxidizing thermal cycling, *Composites Science and Technology* (2007), doi: [10.1016/j.compscitech.2007.10.042](https://doi.org/10.1016/j.compscitech.2007.10.042)

This is a PDF file of an unedited manuscript that has been accepted for publication. As a service to our customers we are providing this early version of the manuscript. The manuscript will undergo copyediting, typesetting, and review of the resulting proof before it is published in its final form. Please note that during the production process errors may be discovered which could affect the content, and all legal disclaimers that apply to the journal pertain.



G. Lubineau, D. Violeau and P. Ladevèze

*LMT-Cachan (E.N.S. de Cachan / Université Paris 6 / C.N.R.S.)*

*61 Avenue du Président Wilson / 94235 CACHAN CEDEX*

*Tel: 33 - 1.47.40.24.02 Fax: 33 - 1.47.40.27.85*

## **Illustrations of a microdamage model for laminates under oxidizing thermal cycling**

---

### **Abstract**

Degradations initiated near the edges of a laminate can have a significant effect on its state of degradation, even at the core. Indeed, results from the literature show that laminates which have the same stress state at the core can have completely different states of degradation, even far away from the edges. The paper discusses the influence of the edge effect on damage initiation and propagation for a specific example. A computational micromechanical approach to the degradation of laminated composites was developed recently at LMT-Cachan. This is a hybrid approach in which, depending on the scale, the mechanisms are described using continuous damage mechanics or finite fracture mechanics. Initially developed for static loading, this technique is being extended to fatigue and environmental effects. The aim of this paper is to illustrate the capability of such an approach to take into account major observations during cyclic loading in an oxidizing atmosphere, even when edge effects are significant.

*Key words:* microcracking, fatigue, damage, micromechanics

---

## 1 Introduction

Today, applications of laminated composites are limited mainly to parts of secondary importance subjected to relatively moderate, almost exclusively mechanical loading.

In the future, these materials will be increasingly used for vital structures subjected to high loads (not only mechanical, but also chemical or physical). Among these new applications are structural parts of the future civilian European supersonic airplane, which was studied as part of the “Supersonic Aeronautical Program” financed by the French Ministry of Equipment and Transportation. In this particular application, the material will be subjected to intensive thermal cycles (four-hour takeoff/landing cycles). In addition to classical fatigue damage, degradation due to the progressive oxidation of the material will also occur because of the relatively high temperature (approximately  $130^{\circ}\text{C}$  at Mach 2.0) and the presence of oxygen. In fact, the degradation process is a much more complex combination of static degradation, fatigue damage and oxidation-induced degradation, resulting in the rapid development of elaborate patterns of degradation, especially microcracking ([1–3]).

The safe dimensioning of these applications requires degradation to be properly described in the vicinity of the critical zones constituted by geometric discontinuities (holes, ply seams, edges in the broad sense). These zones present

---

*Email address:* [lubineau@lmt.ens-cachan.fr](mailto:lubineau@lmt.ens-cachan.fr) (G. Lubineau, D. Violeau and P. Ladevèze ).

difficulties for two reasons:

The first reason is that these zones endure high out-of-plane stresses, whereas away from the edges the structure is mainly in a plane stress state. Interlaminar degradations (mainly delamination) and intralaminar degradations (e.g. microcracking) coexist and are highly coupled near the edges. Taking into account such coupling is currently a scientific challenge for which solutions were proposed only recently.

The second reason is that these zones are where high loading gradients occur. Consequently, while the interior solution varies relatively slowly, significant stress variations take place very locally near the edges, especially in the presence of high thermal stresses. Thus, it is well-known that degradations can be initiated at the edges long before they occur in the core. Moreover, degradations initiated near the edges develop towards the core in an unstable or stable way depending on several parameters, some inherent to the ply (particularly its thickness [4]), others related to the geometry of the sample (e.g. the stacking sequence, which influences the local stress state at the edges directly). If these degradations turn out to be unstable, they propagate towards the core in contradiction with classical laminate theory which would predict no damage. Therefore, in a laboratory sample, edge effects can have a deep impact down to the core. For a structure of industrial complexity, this effect is undoubtedly much more limited, but it is still necessary to predict accurately whether these degradations penetrate or not. In addition to these purely mechanical considerations, the edges play another important role from the physico-chemical point of view because the penetration of oxygen within the existing cracks can be very different depending on the local stress state.

Here, our objective is to show that the hybrid micromechanical model developed recently ([5,6]) is capable of reproducing this significant edge effect and to show that one must take it into account in order to analyze experimental results properly.

The first part of the paper focuses on some recent results from the literature ([3,7]) in which the experimental observations can be explained only by the existence of edge effects. These observations involved comparisons of the states of degradation among samples with identical inner stress states, but with very different edge effects (e.g. identical constitutive plies, but different stacking sequences). The influence of the edges is illustrated in the case of thermomechanical cycling under mechanico-chemical coupling. These results are first discussed through traditional fracture mechanics in order to illustrate clearly the influence of the edge effects on observable degradation.

Therefore, it is necessary to develop a model capable of taking edge effects and their influence on the stable or unstable propagation of degradations towards the core of the sample into account correctly. A hybrid micromechanical model was proposed recently at LMT-Cachan. Initially introduced for static loading ([3,7]), this model was recently extended to include fatigue damage and oxidation effects [8]. A general outline of this model is given in the second part.

Finally, the third part discusses the capability of this model to reproduce the experiments considered. Only preliminary qualitative results are presented here because of the current lack of data for identification. Nevertheless, we show that our model is capable of capturing the key features of the experimental observations for this difficult problem.

## 2 Experimental observation of cyclic results: presentation and analysis

Here, we discuss the experimental results of [7], which are summarized in Figure 1 and concern pure thermal cycles  $[-50\text{C}/150\text{C}]$  (triangular cycles  $4/\text{min}$ ) on  $35 * 25 \text{ mm}^2$  rectangular samples of IM7/977-2 composite (cf. [7] for details of the experimental procedure). The stacking sequences were  $[-45_3/+45_3]_s$  and  $[0_3/90_3]_s$ , and the samples were cycled under different environments: neutral atmosphere (pure dry nitrogen) and oxidizing atmosphere (pure dry oxygen).

[Fig. 1 about here.]

Under such loading, the stresses in the core of each sample are due only to the differential expansion between the plies and are, of course, the same for the two stacking sequences. Therefore, a simple analysis based on the local stress state within the core would lead to similar interior degradations. However, the observations of Figure 1 clearly show that microcracks occur within the core of the central ply for the  $[0_3/90_3]_s$  while the central ply of the  $[-45_3/+45_3]_s$  remains completely healthy. In a neutral atmosphere, this difference must be explained only by mechanical considerations. The results also show that this difference between the two sequences is amplified by oxidation.

The only reasonable explanation for these major differences lies in the edge effect, which is the only difference between the two sequences under this type of loading. Therefore, it is necessary to carry out a more precise analysis of the coupling among the edge effect, the microcracking state and oxidation,

even within the core.

### 2.1 Influence of the edge effect on the energy release rate

First, for both sequences, let us consider the evolution of the energy release rate of a transverse microcrack during its propagation from the edge towards the core. In both cases, the crack's growth was simulated by finite elements (see Figure 2) under the assumption of a periodic microcracking pattern in the direction of the edge. The reference loading was a global  $\Delta T = -100C$  temperature variation. In addition, the problem was assumed to be linear elastic.

[Fig. 2 about here.]

The energy release rates corresponding to the growth of the microcrack from edge to core were calculated by virtual crack extension. The results are shown in Figure 3.

[Fig. 3 about here.]

For long cracks, the curves tend towards a common value because the stress state of the interior solution is the same in both cases and corresponds to the steady-state value classically obtained by 2D analysis under the assumption of an infinite microcrack [9–11] . . . However, one can observe completely different types of behavior at the edge of the samples. In the  $[-45_3 / +45_3]_s$  sample, initiation is greatly delayed. Consequently, even if the core energy release rates of the two samples are identical, microcracking cannot develop in the

$[-45_3/+45_3]_s$  because initiation does not occur, whereas it can propagate extensively in the  $[0_3/90_3]_s$ .

## 2.2 Influence of the edge effect on the crack's opening

The edge effect also modifies the opening of the potential oxidation path. The local opening of the cracks for the two sequences is shown in Figure 4.

[Fig. 4 about here.]

In the steady-state solutions (long cracks far from the edges), the opening tends to be the same for the two sequences. But the edge effect limits the penetration of oxygen in the  $[-45_3/+45_3]_s$  compared to the  $[0_3/90_3]_s$  case. This is especially true for very short cracks (see Case A /  $\frac{\Lambda}{H} = 0.2$ , Figure 4). Consequently, not only is crack initiation delayed from a mechanical point of view (Figure 3), but weakening of the material due to oxidation is also limited.

## 3 Bases of the micromechanical model for laminates

The computational damage micromodel for laminates was introduced in [5]. Its material foundations were detailed in [6]: therefore, we will merely review its main concepts, and more particularly its first extensions to fatigue and oxidizing degradation. The objective of this theory is to propose a micromechanical model of the classical elementary mechanisms which could be used as a reference material under general loading. In that sense, it differs greatly from classical micromechanical approaches, which would describe only some

specific mechanisms under some specific loading type.

Let us first recall that we assume that any complex state of degradation of a laminated composite can be described as the result of the development of four basic mechanisms: two diffuse mechanisms (one for the ply and one for the interface), and two discrete mechanisms on the ply's scale (transverse microcracking and induced local delamination at the interface). A more detailed description of these mechanisms can be found in [6].

### *3.1 The hybrid micromechanical model under static loading*

The first key step consists in grouping the mechanisms according to their characteristic scales. On the scale of the elementary ply, diffuse intra- and interlaminar damage can be considered locally homogeneous, whereas transverse microcracks and diffuse delamination can be associated with clear fracture surfaces. This leads to the following choice: the degradation of the fiber-matrix material is described using the classical continuum mechanics framework, while transverse microcracking and local delamination are described using a discrete approach based on a generalization of finite fracture mechanics [12].

#### *3.1.1 Continuous damage mechanics for the progressive mechanisms*

For the description of damage associated with fiber/matrix debonding and small cracks within the matrix connecting close fibers, the classical form of the

damage mesomodel ([13], [14]) was retained. Let 1 denote the fiber's direction, 2 the in-plane transverse direction and 3 the out-of-plane transverse direction.

In the elementary ply, for instance, the damaged material is assumed to remain transverse isotropic and its state is classically described by two damage variables: one in the transverse direction (denoted  $\tilde{d}'$ ), and one in the shear direction (denoted  $\tilde{d}$ ). These variables are assumed to be constant throughout the thickness of the mesoconstituent. Following that assumption, the evolution of damage is expressed as a function of the damage forces  $\tilde{Y}_{\tilde{d}}$  and  $\tilde{Y}_{\tilde{d}'}$ :

$$\begin{aligned}\tilde{d} &= \sup_{\tau \leq t} \left[ \frac{\sqrt{\tilde{Y}_{\tilde{d}} + b_2 \tilde{Y}_{\tilde{d}'} - \sqrt{Y_0}}}{\sqrt{Y_c}} \right] \\ \tilde{d}' &= b_3 \tilde{d}\end{aligned}\tag{1}$$

where  $b_2$ ,  $b_3$ ,  $Y_c$  and  $Y_0$  are material coefficients identified experimentally. Since the damage variables are assumed to be constant throughout the thickness of the single layer, the constitutive relation involves mean values of the damage forces throughout the thickness, so that:

$$\begin{aligned}\tilde{Y}_{\tilde{d}'} &= \left\langle \left\langle \frac{(\sigma_{22})_+^2}{2E_2^0(1-\tilde{d}')^2} \right\rangle \right\rangle \\ \tilde{Y}_{\tilde{d}} &= \left\langle \left\langle \frac{\sigma_{12}^2}{2G_{12}^0(1-\tilde{d})^2} \right\rangle \right\rangle\end{aligned}\tag{2}$$

where  $\langle \langle \cdot \rangle \rangle$  and  $\langle \cdot \rangle_+$  denote the mean value throughout the thickness and the positive part respectively, in order to distinguish the behavior in traction (where cracks are active) from the behavior in compression (where cracks are assumed to be closed).

### 3.1.2 Finite fracture mechanics for cracking and delamination

The surfaces of the cracks are described using a discrete approach. Thus, the complex cracking pattern is assumed to occur within the structure through the accumulation of complete breakage of elementary surfaces, whose areas are determined from micromechanical considerations [6]. Consequently, the area of each type of surface defines the minimum amount of degradation considered in our approach. Thus, the mechanisms of degradation are quantified, which guarantees that our approach behaves well in terms of localization.

Two types of surfaces must be considered. The first type refers to the intralaminar surfaces, which are assumed to be parallel to the fibers and represent transverse cracking. The second type refers to interlaminar surfaces, which represent local delamination. Whatever the nature of a surface, its failure is governed by a discrete energy criterion. Consequently, the basic material quantities involved in the model are the critical energy release rates  $\{\bar{G}_c\}$ , designated for each mode by  $\{\bar{G}_{c-p}^{I,II,III}\}$  for the ply and  $\{\bar{G}_{c-i}^{I,II,III}\}$  for the interface. A surface breaks when its damage force reaches its critical energy release rate. When this happens, friction is introduced.

The damage forces for intralaminar cracks are defined as follows:

- at initiation (failure of an isolated surface):

$$\{G_i\} = \min\left[h \cdot \frac{\{\Delta G\}}{h}; \bar{h} \cdot \frac{\{\Delta G\}}{h}\right] \quad (3)$$

- during propagation (failure of a surface adjacent to a previously cracked

surface):

$$\{G_p\} = \{\Delta G\} \quad (4)$$

where  $\Delta G$  is the discrete energy release rate associated with complete breakage of the surface. Thus,  $\Delta G$  is a mean value of the classical continuous energy release rate:

$$\Delta G = \frac{\int_a^{a+\Delta a} G(a) \delta a}{\Delta a} \quad (5)$$

where  $\Delta a$  is the prescribed minimum cracking surface. The discrete values of  $\Delta G$  for the crack growth shown in Figures 2 and 3 are plotted in Figure 5. One can note that the edge effect is taken into account in an average sense.

[Fig. 5 about here.]

$\bar{h}$  is a critical thickness characteristic of the material (typically of the order of twice the thickness of the elementary material ply) and  $h$  is the thickness of the unidirectional layer.

### 3.2 Extension to fatigue damage and environmental effects

In our approach, critical energy release rates are introduced explicitly in the analysis of the structure. A relatively easy means of introducing fatigue damage and environmental effects consists in assuming that they affect these critical quantities alone. At the same time, transverse microcracking and local delamination are assumed to remain governed by the static degradation law

defined in 3.1.2. Thus, discrete mechanisms develop naturally within the structure due to the local reduction of tenacities and the verification of the static degradation law. This approach was described in [8], and is briefly reviewed below.

Two internal variables are introduced:  $\eta_f$  which represents the fatigue damage effect, and  $\eta_{ox}$  which, in our case, represents the oxidation effect. Thus, the current critical energy release rate of the material is:

$$\{G_c\} = \{\bar{G}_c\} \cdot (1 - \eta_f) \cdot (1 - \eta_{ox}) \quad (6)$$

An intrinsic constitutive relation for the calculation of  $\eta_f$  is defined as a more or less complex function  $\mathcal{F}$  of the local damage forces:

$$\frac{\partial \eta_f}{\partial N} = \mathcal{F}(\tilde{Y}_{\tilde{d}}, \tilde{Y}_{\tilde{d}'}) \quad (7)$$

(A first tentative identification of  $\mathcal{F}$  under transverse loading can be found in [8].)

Concerning oxidation, only active surfaces are assumed to be affected. A surface is considered to be active if it is in direct contact with the atmosphere (through the skin, the edges or the cracks). If a surface becomes active with respect to oxidation, its critical energy release rate decreases immediately depending on the temperature and the partial oxygen pressure.

#### 4 Examples using the computational micromodel

Let us consider the numerical example of an octagonal  $[0_3/90_6/0_3]$  sample studied in [7]. Since this structure includes fibers at both 90 and 45 degrees with respect to the edges, it combines the results of the rectangular  $[0_3/90_6/0_3]$  and  $[45_3/-45_3/45_3]$  samples already studied in 2. The same thermomechanical cycling in an oxidizing atmosphere applied to this sample results in a complex degradation pattern (Figure 6 [a]) which clearly presents the edge effects discussed in Parts 2.1 and 2.2.

[Fig. 6 about here.]

Because of symmetry, only one-quarter of the sample was retained for the calculation (Figure 6 [b]). In order to comply with our micromechanical model, each ply was divided *a priori* into homogeneous elementary volumes (in which diffuse damage can develop) and interfaces (which, depending on their orientation, represent transverse microcracking or local delamination). This choice of introducing potentially cracked areas *a priori* was made for the sake of simplicity: improved strategies involving the dynamic occurrence of crack surfaces could certainly be derived, but this would require some programming which has not yet been done. Each elementary volume was meshed in three dimensions, leading to a large number of degrees of freedom: in other words, the approach proposed is relatively simple from the “modeling” point of view, but requires powerful computation capabilities. Therefore, multiscale computational strategies must be developed and used for such problems. The resolution performed here, which will be detailed in further publications, was based on the approach proposed at LMT-Cachan ([15,16]).

At this point, due to the lack of experimental results which would allow the complete identification of the model, the results are purely qualitative. The identification of the model will be the subject of forthcoming works. Therefore, our comparisons will not be made in terms of quantitative results (e.g. evolution of the density of cracks as a function of the number of cycles), but only in terms of the morphology of the degradations observed.

[Fig. 7 about here.]

Figure 7 shows the progressive evolution of the cracking pattern within the central ply of the sample. It appears clearly that the main characteristics of the experimental results are correctly reproduced:

- as observed classically in fatigue tests ([17–21]), microcracks develop first near the edge of the sample until saturation of the microcracking rate. Then, cracks propagate from the edge toward the core. Let us note that in our approach the initiation and propagation of cracks are governed by the reduction of the critical energy release rate. This reduction is due to the development of both  $\eta_f$  (for the fatigue part) and  $\eta_{ox}$  (for the oxidation part). Contrary to classical micromechanical modeling, no specific mechanism is introduced in the model to describe the multiplication near the edges and the growth towards the core, which seems satisfactory because, then, there is only one underlying physics.
- the influence of the edge effect is correctly accounted for. As observed experimentally, there is no crack starting from the 45-degree edge. The profile of the fracture criterion for Illustration 7-7 is shown in Figure 8. Even though the criterion is approximately homogeneous within the core, cracks which are not initiated along the 45-degree edge cannot appear in the core, whereas

cracks initiated along the 90-degree edge propagate extensively.

[Fig. 8 about here.]

## 5 Conclusions and prospects

We studied the well-known and major role of edge effects in the degradation of laminates using fracture mechanics. Very different states of degradation can be observed away from the edges, even among samples having the same interior stress state. We showed that this can be explained as the result of the propagation of degradations initiated near the edges, which can be stable or unstable.

The computational micromechanical model proposed in previous works is able to predict this edge influence qualitatively, even in complex situations such as fatigue loading in an oxidizing atmosphere. Additional work is necessary in order to improve the identification part of this approach and end up with a predictive tool.

## References

- [1] H. McManus, D. Bowles, S. Tompkins, Prediction of thermal cycling induced matrix cracking, *Journal of Reinforced Plastics and Composites* 15 (1996) 124–140.
- [2] S. Kobayashi, K. Terada, S. Ogihara, N. Takeda, Damage-mechanics analysis of matrix cracking in cross-ply cfrp laminates under thermal fatigue, *Composites Sciences and Technology* 61 (2001) 1735–1742.
- [3] M. Lafarie-Frenot, S. Rouquie, Influence of oxidative environments on damage

- in c/epoxy laminates subjected to thermal fatigue, *Composites Sciences and Technology* 64 (2004) 1725–1735.
- [4] L. Boniface, P. Smith, M. Bader, A. Rezaifard, Transverse ply cracking in cross-ply cfrp laminates. initiation or propagation controlled, *Journal of Composite Materials* 31 (11) (1997) 1080–1112.
- [5] P. Ladevze, Multiscale computational damage modelling of laminate composites, in: Taljera-Manson (Ed.), *Course CISM*, 2005, accepted, in press.
- [6] P. Ladevze, G. Lubineau, D. Violeau, A computational damage micromodel of laminated composites, *International Journal of Fracture* 137 (1-4) (2006) 139–150.
- [7] M. Lafarie-Frnot, N. Ho, Influence of free edge intralaminar stresses on damage process in cfrp laminates under thermal cycling conditions, *Composites Sciences and Technology* In press, Corrected Proof, Available online 3 November 2005.
- [8] G. Lubineau, P. Ladevze, D. Violeau, Durability of cfrp laminates under thermomechanical loading: A micro-meso damage model, *Composites Science and Technology* 66 (1-4) (2006) 983–992.
- [9] J. Nairn, S. Hu, Matrix microcracking, in: Taljera (Ed.), *Damage Mechanics of Composite Materials*, 1994, pp. 187–243.
- [10] J. Nairn, Matrix microcracking in composites, in: Taljera-Manson (Ed.), *Polymer Matrix Composites*, *Comprehensive Composite Materials*, Ch.13, Elsevier Science, 2000, pp. 403–432.
- [11] S. Ho, Z. Suo, Tunneling cracks in constrained layers, *Journal of Applied Mechanics* 60 (1993) 890–894.
- [12] Z. Hashin, Analysis of cracked laminates: a variational approach, *Mechanical of Materials* 4 (1985) 121–136.

- [13] P. Ladevèze, E. LeDantec, Damage modeling of the elementary ply for laminated composites, *Composites Science and Technology* 43 (3) (1992) 257–267.
- [14] O. Allix, P. Ladevèze, Interlaminar interface modelling for the prediction of laminate delamination, *Composite Structures* 22 (1992) 235–242.
- [15] P. Ladevze, O. Loiseau, D. Dureisseix, A micro-macro and parallel computational strategy for highly heterogeneous structures, *Int. J. for Numerical Methods in Engineering* 52 (2001) 121–138.
- [16] P. Ladevze, A. Nouy, On a multiscale computational strategy with time and space homogenization for structural mechanics, *Computer Methods in Applied Mechanics* 192 (2003) 3061–3087.
- [17] L. Boniface, S. Ogin, Application of the paris equation to the fatigue growth of transverse ply cracks, *Journal of Composite Materials* 23 (1989) 735–754.
- [18] T. Yokozeki, T. Aoki, T. Ishikawa, Fatigue growth of matrix cracks in the transverse direction of cfrp laminates, *Composites Science and Technology* 62 (2002) 1223–1229.
- [19] L. Boniface, P. Smith, S. Ogin, M. Bader, Observations on tranverse ply crack growth in a  $[0/90_2]_s$  CFRP laminate under monotonic and cyclic loading, *P6ICCM* 3 (1987) 156–165.
- [20] J. Berthelot, Transverse cracking and delamination in cross-ply glass-fiber and carbon-fiber reinforced plastic laminates: static and fatigue loading, *Appl. Mech. Rev.* 56 (1) (2003) 1–37.
- [21] J. Berthelot, Transverse cracking and delamination in cross-ply laminates under static and fatigue loadings, *Applied Mechanics Reviews* 56 (2003) 111–147.

## List of Figures

- |   |  |    |
|---|--|----|
| 1 | X-ray pictures of rectangular specimens after 1,000 thermal cycles $[-50/150C]$ in nitrogen and oxygen (from [7])  | 19 |
| 2 | Simulation of the periodic propagation from edge to core. A microcracking rate $\rho = 0.5$ was used for the example ( $\rho = \frac{H}{L}$ , $H$ being the thickness of the ply and $L$ the mean distance between cracks)       | 20 |
| 3 | Evolution of the energy release rate for $[0_3/90_3]_s$ and $[-45_3/+45_3]_s$ laminates under pure thermal loading   | 21 |
| 4 | Local crack opening for short and long cracks in $[0_3/90_3]_s$ and $[-45_3/+45_3]_s$ (pure reference thermal loading $\Delta T = -100C$ , periodic cracking pattern $\rho = 0.5$ )  | 22 |
| 5 | Evolution of the discrete energy release rate for $[0_3/90_3]_s$ and $[-45_3/+45_3]_s$ laminates under pure thermal loading. The length of the crack was discretized with a step equal to the thickness of the elementary layer. | 23 |
| 6 | X-ray pictures of the octagonal specimen after 1,000 $(-50^\circ C/150^\circ C)$ cycles in oxygen (from [7])   | 24 |
| 7 | Evolution of the simulated pattern of microcracks under thermomechanical cycling with oxidizing atmosphere (central ply of the octagonal sample)   | 25 |
| 8 | Illustration of the profile of the fracture criterion (a surface fails when the criterion is equal to 1)   | 26 |

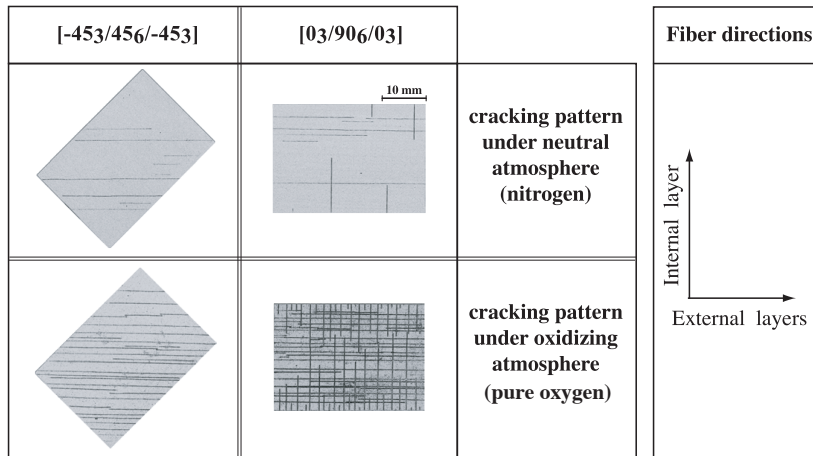


Fig. 1. X-ray pictures of rectangular specimens after 1,000 thermal cycles  $[-50/150C]$  in nitrogen and oxygen (from [7])

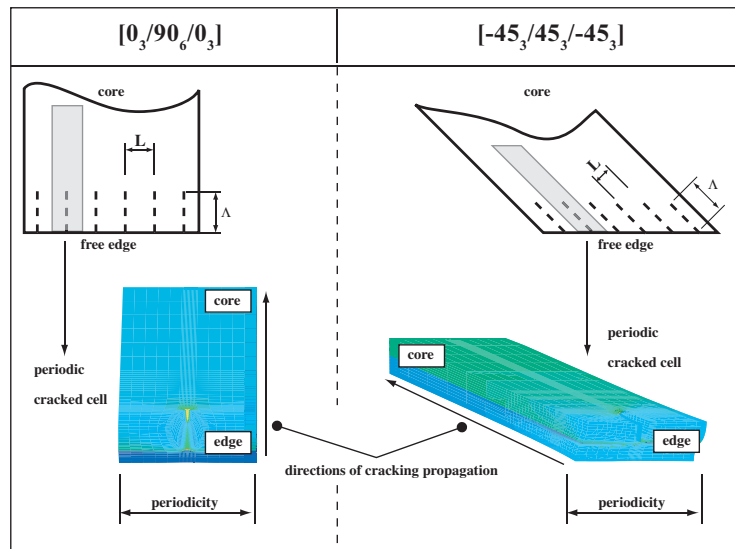


Fig. 2. Simulation of the periodic propagation from edge to core. A microcracking rate  $\rho = 0.5$  was used for the example ( $\rho = \frac{H}{L}$ ,  $H$  being the thickness of the ply and  $L$  the mean distance between cracks)

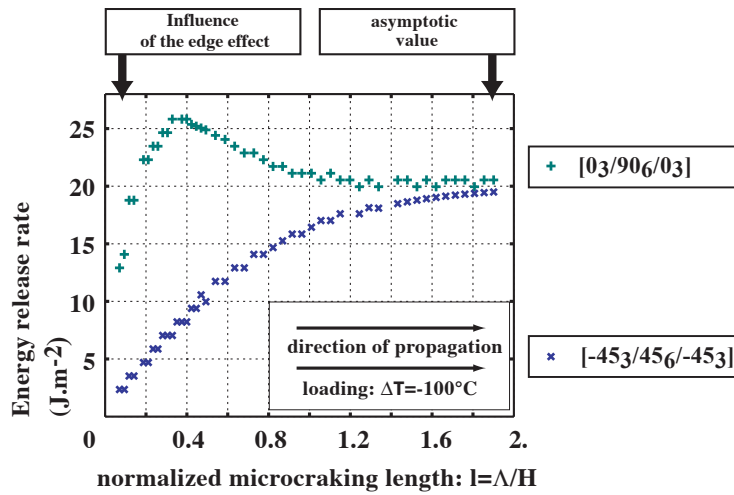


Fig. 3. Evolution of the energy release rate for  $[0_3/90_3]_s$  and  $[-45_3/+45_3]_s$  laminates under pure thermal loading

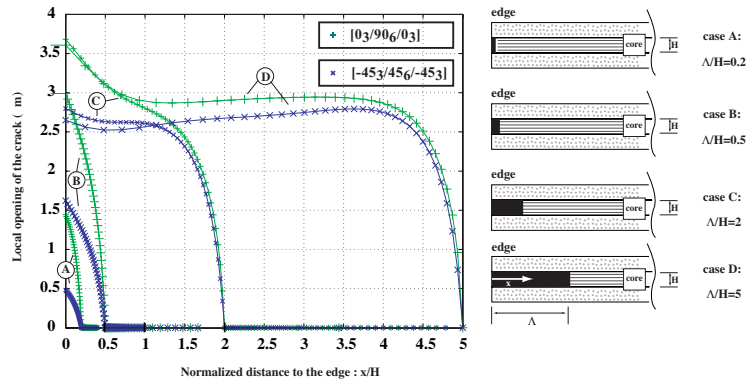


Fig. 4. Local crack opening for short and long cracks in  $[0_3/90_3]_s$  and  $[-45_3/+45_3]_s$  (pure reference thermal loading  $\Delta T = -100C$ , periodic cracking pattern  $\rho = 0.5$ )

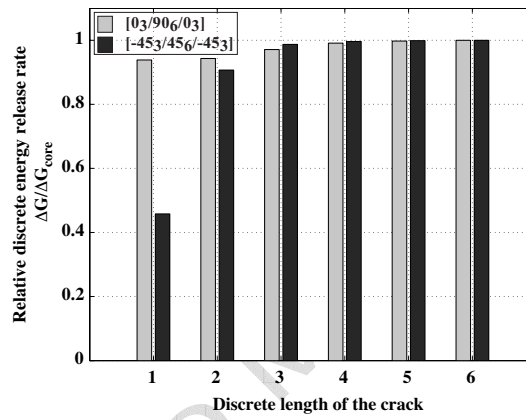


Fig. 5. Evolution of the discrete energy release rate for  $[0_3/90_3]_s$  and  $[-45_3/+45_3]_s$  laminates under pure thermal loading. The length of the crack was discretized with a step equal to the thickness of the elementary layer.

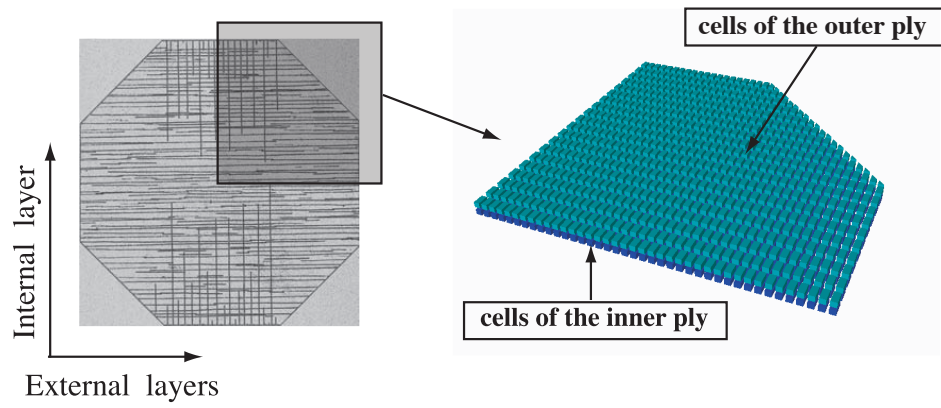


Fig. 6. X-ray pictures of the octagonal specimen after 1,000 ( $-50^{\circ}C/150^{\circ}C$ ) cycles in oxygen (from [7])

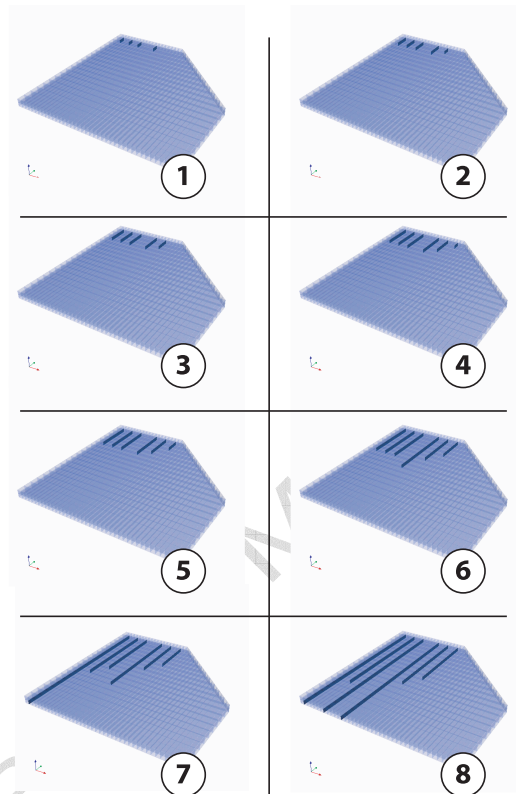


Fig. 7. Evolution of the simulated pattern of microcracks under thermomechanical cycling with oxidizing atmosphere (central ply of the octagonal sample)

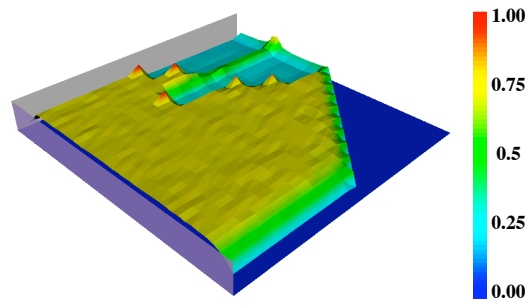


Fig. 8. Illustration of the profile of the fracture criterion (a surface fails when the criterion is equal to 1)

ACCEPTED MANUSCRIPT